

## HIGH-TEMPERATURE PROPERTIES OF Fe<sub>3</sub>Al WITH ADDITION OF 2 AT.% OF Zr

KEJZLAR Pavel<sup>1</sup>, ŠVEC Martin<sup>2</sup>

<sup>1</sup>Technical University of Liberec, Institute for Nanomaterials, Advanced Technologies and Innovation, Liberec, Czech Republic, EU

<sup>2</sup>Technical University of Liberec, Department of Material Science, Liberec, Czech Republic, EU

### Abstract

Iron aluminides are perspective structural materials for high temperature use. Addition of Zr into Fe<sub>3</sub>Al matrix leads to formation of strengthening intermetallic phases, which affect their high-temperature behaviour. The present work focuses on the behavior at high temperature, especially on the mechanical strength and coefficient of thermal expansion with respect to the alloy structure. Transition temperatures are not affected by Zr-addition in comparison to binary alloy.

**Keywords:** Intermetallics, iron aluminides, structure, coefficient of thermal expansion, yield stress

## 1. INTRODUCTION

### 1.1. Iron aluminides

Iron aluminides are perspective as structural materials for high temperature use because they exhibit some beneficial properties. Together with low price and easy availability of raw materials are especially favourable stiffness-to-weight ratio and excellent oxidation resistance. However, these intermetallic materials suffer from their low to medium temperature brittleness and insufficient high temperature strength [1-3]. One of the possible ways to increase the high temperature mechanical properties is addition of the ternary element into binary Fe-Al alloy [4, 5]. Mechanical strengthening can occur in four basic ways:

- By the solid solution hardening
- Precipitation of coherent ternary phase
- Precipitation of incoherent particles
- By the stabilization of ordered structure to higher temperatures

An equilibrium binary Fe-Al diagram is showed in **Fig. 1**.

### 1.2. Fe-Al-Zr alloys

It has been shown that addition of already small amount of zirconium into Fe<sub>3</sub>Al or Fe-Al based alloy leads to formation of hard and thermally stable phases [6-8]. Two equilibrium ternary phases were described -  $\lambda_1$  Laves phase with hexagonal lattice (Fe,Al)<sub>2</sub>Zr and  $\tau_1$  phase (Fe,Al)<sub>12</sub>Zr (see ternary Fe-Al-Zr diagram in **Fig. 2**) [9]. High temperature mechanical tests shown that presence of both,  $\lambda_1$  and  $\tau_1$  phase, can effectively increase the high temperature strength at temperatures around 700 °C [7,8,10,11]. Therefore, through the suitable choice of the composition can be achieved the structure consisting of a ductile Fe-Al phase and Laves- or  $\tau_1$ -phase. These intermetallic phases can significantly affect the high temperature mechanical properties due to their hardness and thermal stability.

### 1.3. Coefficient of thermal expansion

Not only the high temperature strength but also coefficient of thermal expansion (CTE) is key parameter for designers and engineers. It is necessary to be reckoned with a change of dimensions caused due to the thermal expansion in application of these materials at high temperatures for which they are intended. Current research deals with the structure, mechanical properties, oxidation and corrosion behaviour, however in the

literature there are only few mentions about the coefficient of thermal expansion of iron aluminides. The CTE depends on the temperature and on the structure. The measurement of CTE gives us information not only about change of the dimensions, but also about structural and phase transformations and helps us to understand better the behaviour of alloys at high temperatures.

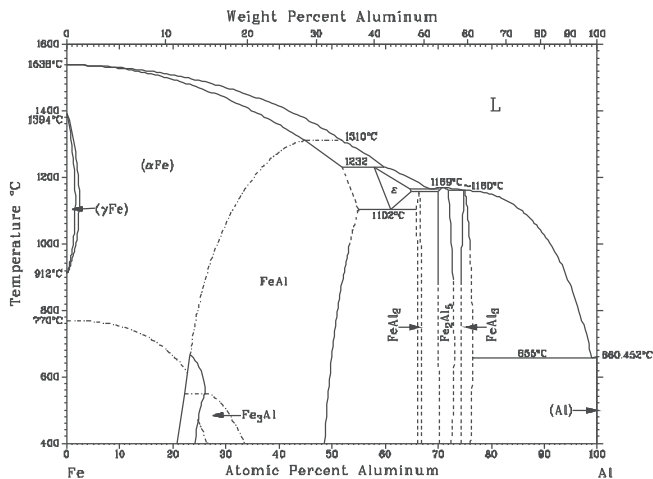


Fig. 1 Fe-Al binary diagram [3]

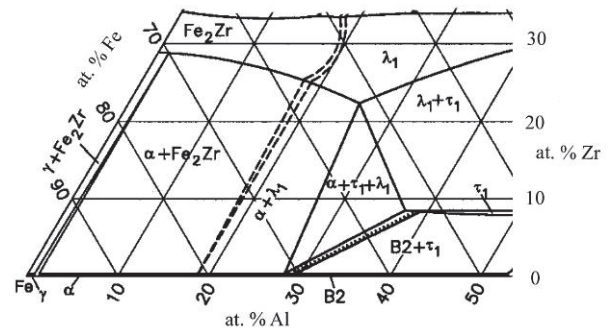


Fig. 2 Fe-rich part of isothermal section of Fe-Al-Zr diagram at 1000 °C [9].

## 2. EXPERIMENTAL METHODS

### 2.1. Sample preparation

The investigated alloys were melted in vacuum and casted. The alloys nominal composition was Fe-25Al-2Zr and Fe-30Al-2Zr (at.%). Concentrations of impurities coming from raw materials were lower than 0.1 at.% Cr; 0.01 at.% B; 0.1 at.% Mn; 0.06 at.% C. Samples for metallographic structure description were electrochemically polished using LectroPol-5 (Struers) with A2 electrolyte. The dimensions of samples used for high temperature compression test were 6 x 6 x 10 mm. For the samples preparation was used EDM. The prismatic samples with dimensions of 7 x 7 x 15 mm were cut from bulk by the use of precision saw for the CTE measurement. The surface of samples for compression test and CTE measurement was carefully polished using sandpaper grit #1200.

### 2.2. Structure

Structure was observed using a field emission scanning electron microscope Zeiss Ultra Plus equipped with EDS detector Oxford X-Max for local chemical microanalysis and EBSD detector Oxford NordlysNano for determination of phase crystal structure. The structure was examined in the initial (as cast) state and after CTE thermal cycle.

### 2.3. High temperature mechanical properties

High temperature mechanical properties were assessed using compression test. Deformations were carried out by digitally controlled testing machine (INSTRON 1186) at temperatures of 600, 700, 800 and 880 °C. Compression tests were performed with a strain rate of  $1.5 \cdot 10^{-4} \text{ s}^{-1}$ , the temperature was kept with the accuracy of 3 °C.

### 2.4. Coefficient of thermal expansion

Thermal expansion was measured using a horizontal dilatometer. During the measurement the samples were placed into a holder of dilatometer and the whole system was inserted in the furnace. The heating rate was 4 °C/min. CTEs were calculated according to equation:

$$\alpha_T = \frac{l_T - l_0}{T - T_0} \cdot \frac{1}{l_0} \quad (1)$$

where  $\alpha_T$  = coefficient of thermal expansion;  $l_T$  = length of the sample at given temperature;  $l_0$  = length of the sample at laboratory temperature (20 °C),  $T$  = applied temperature;  $T_0$  = laboratory temperature. CTE curves were recorded in the temperature range from 400 to 1200 °C.

### 3. RESULTS

#### 3.1. Structure

The initial (as cast) structures are shown in **Figs. 3** and **4**. The matrix of both alloys is Fe<sub>3</sub>Al with a fine lamellar eutectic composed of Fe<sub>3</sub>Al +  $\lambda_1$  Laves phase. The structures after thermal cycle are in **Figs. 5** and **6**. A coagulation of Laves phase (**Fig. 5**) was observed after the dilatation cycle in the case of Fe-25Al-2Zr. In **Fig. 6** there is a structure of Fe-30Al-2Zr. In addition to the coarsening a partial phase transformation of Laves phase to  $\tau_1$  phase occurred ( $\tau_1$  appears as light grey areas).

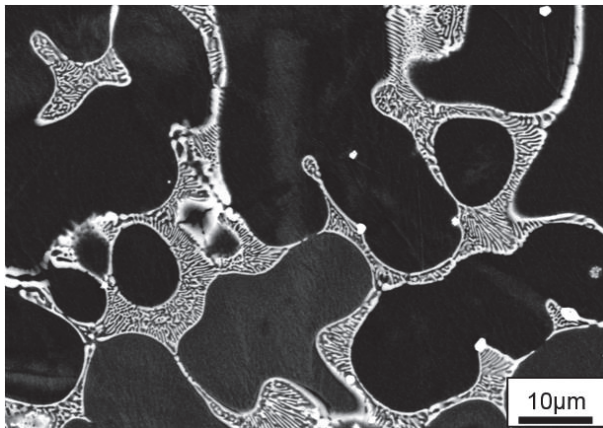


**Fig. 3** The microstructure of Fe-25Al-2Zr alloy in the initial state (as cast). The structure is composed of a dark Fe<sub>3</sub>Al matrix and a lamellar eutectic Fe<sub>3</sub>Al +  $\lambda_1$

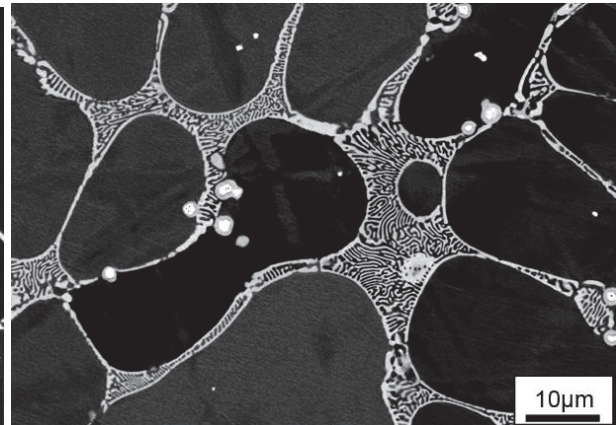


**Fig. 4** The structure of Fe-30Al-2Zr sample in as cast state is the same as Fe-25Al-2Zr

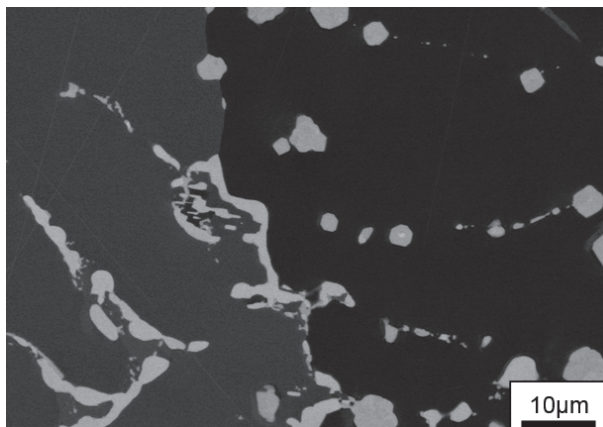


**Fig. 5** The structure of Fe-25Al-2Zr after dilatation cycle. Coarse  $\lambda_1$  particles in Fe<sub>3</sub>Al matrix are visible

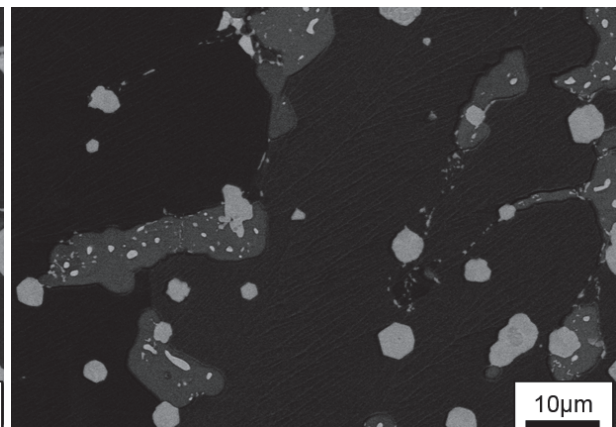


**Fig. 6** The structure of Fe-30Al-2Zr sample after dilatation cycle. A part of  $\lambda_1$  phase transformed to  $\tau_1$ , the rest of Laves phase coarsened

### 3.2. Mechanical properties

The graph in **Fig. 7** shows the dependence of  $R_{p0.2}$  yield stress on the temperature. A positive effect of a higher Al concentration is visible. The values of yield stress steeply and nonlinearly decrease with increasing temperature.

### 3.3. CTE

The dependence of coefficient of thermal expansion on the temperature is in **Fig. 8**. Both curves show two changes in their slope. The first part corresponds to  $D0_3$ . Phase transformation  $D0_3 \rightarrow B2$  took place around 560 °C. The B2 structure is stable up to 780 °C for Fe<sub>25</sub>Al<sub>2</sub>Zr alloy; in the case of the Fe<sub>30</sub>Al<sub>2</sub>Zr alloy, it remains stable up to a temperature of 1000 °C where B2 transforms to disordered  $\alpha$ Fe lattice.

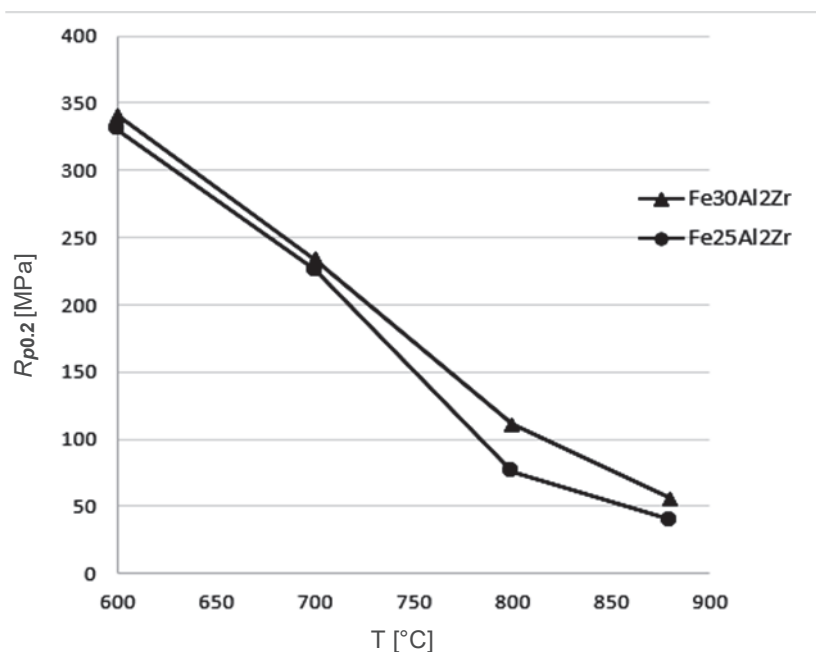


**Fig. 7** Dependence of yield stress on temperature

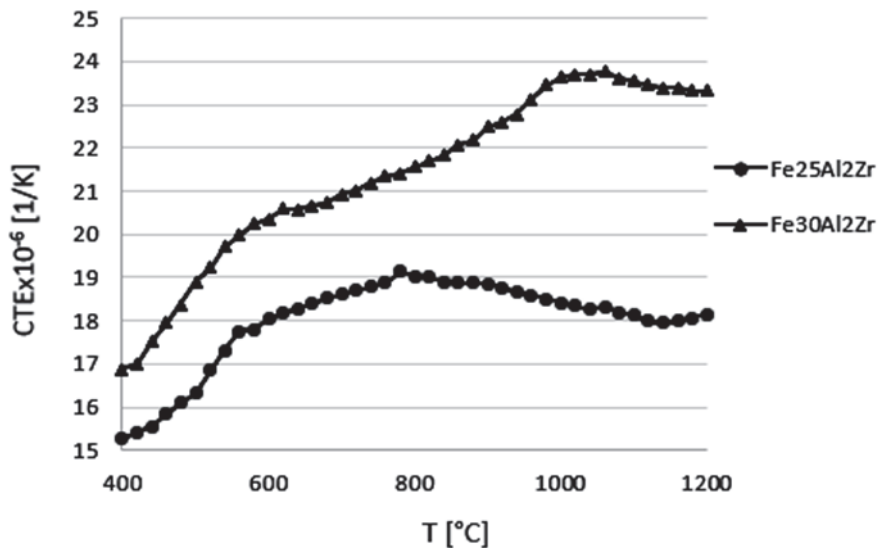


**Fig. 8** Calculated CTE curves. The steepest increase corresponds to  $D0_3$  lattice, middle part is B2 and decrease of CTE with growing temperature was observed for disordered  $\alpha$ Fe lattice

#### 4. DISCUSSION AND CONCLUSIONS

In the initial state (as cast) the structure of both alloys was composed of a Fe<sub>3</sub>Al matrix with a lamellar eutectic  $\lambda_1 + \text{Fe}_3\text{Al}$  (**Figs. 3-4**). The lamellar eutectic coarsened during the CTE temperature cycle (**Fig. 5**) and in the case of alloy Fe<sub>30</sub>Al<sub>2</sub>Zr the Laves phase undergone a partial transformation to the  $\tau_1$  phase (**Fig. 6**) according to ternary Fe-Al-Zr diagram (**Fig. 2**) [9].

Due to very limited solubility of Zr in Fe-Al matrix (< 0.1 %) nearly all Zr formed hard intermetallic phases and thus does not affect matrix phase transition temperatures significantly. Therefore, the measured phase transformations temperatures correspond to the values that can be deduced from the binary Fe-Al diagram (**Fig. 1**) [3]. Increase in Al-content stabilizes the B2 lattice to higher temperature what is beneficial for a high temperature mechanical strength (**Fig. 7**). The steepest increase in CTE with temperature was observed in D0<sub>3</sub> lattice. Slower increase of CTE values shows B2 lattice. A decrease of CTE with temperature was observed for disordered A2 lattice corresponding to  $\alpha\text{Fe}$ . It is worth to notice that with respect to the high temperature strength, this type of alloys is usable up to  $\approx 800$  °C. From the obtained CTE data (**Fig. 8**) it seems that CTE grows with Al concentration. The temperatures of the matrix phase transitions are not affected by Zr addition. However, it should be taken into account that during the applied CTE thermal cycle occurs a wide range of interactions (phase transformation, Laves phase coarsening, surface oxidation...) that's why further studies are necessary to properly understand the CTE.

#### ACKNOWLEDGEMENTS

*The results of this project LO1201 were obtained with co-funding from the Ministry of Education, Youth and Sports as part of targeted support from the "Národní program udržitelnosti I" programme.*

#### REFERENCES

- [1] MCKAMEY C.G., DEVAN J.H., TORTORELLI P.F., SIKKA V.K. A review of recent development in Fe<sub>3</sub>Al-based alloys. Journal of Materials Research, Vol. 6, No. 8, 1991, pp. 1779-1804.
- [2] STOLOFF N.S. Iron aluminides: present status and future prospects. Materials Science and Engineering A, Vol. 258, 1998, pp. 1-14.
- [3] STOLOFF N.S., LIU C.T. Iron aluminides. [editor] Li J.C.M. Microstructure and properties of materials (Vol. 2). Singapore: World Scientific Publishing Co. Ptc. Ltd., 2000, pp. 139-176.
- [4] MORRIS D.G. Possibilities for high-temperature strengthening in iron aluminides. Intermetallics, Vol. 6, 1998, pp. 753-758.
- [5] PALM M. Concepts derived from phase diagram studies for the strengthening of Fe-Al-based alloys. Intermetallics, Vol. 13, 2005, pp. 1286-1295.
- [6] WASILKOWSKA A., BARTSCH M., STEIN F., PALM M., SZTWIERTNIA K., SAUTHOFF G., MESSERSCHMIDT U. Plastic deformation of Fe-Al polycrystals strengthened with Zr-containing Laves phases I. Microstructure of undeformed materials. Materials Science and Engineering A, Vol. 380, 2004, pp. 9-19.
- [7] A. WASILKOWSKA, M. BARTSCH, F. STEIN, M. PALM, K. SZTWIERTNIA, G. SAUTHOFF, U. MESSERSCHMIDT. Plastic deformation of Fe-Al polycrystals strengthened with Zr-containing Laves phases Part II. Mechanical properties. Materials Science and Engineering A, Vol. 381, 2004, pp. 1-15.
- [8] STEIN F., PALM M., SAUTHOFF G. Mechanical properties and oxidation behaviour of two-phase iron aluminium alloys with Zr(Fe,Al)<sub>2</sub> Laves phase or Zr(Fe,Al)<sub>12</sub>  $\tau_1$  phase. Intermetallics, Vol. 13, 2005, pp. 1275-1285.
- [9] STEIN F., SAUTHOFF G., PALM M. Phases and phase equilibria in the Fe-Al-Zr system. Z. Metallkd. 95, 2004, pp. 469-485
- [10] KRATOCHVÍL P., KEJZLAR P., KRÁL R., VODIČKOVÁ V. The effect of Zr addition on the structure and high temperature strength of Fe-30 at.% Al alloys. Intermetallics, Vol. 20, 2012, pp. 39-46.
- [11] KEJZLAR P., KRATOCHVÍL P., KRÁL R., VODIČKOVÁ V. Phase structure and high-temperature mechanical properties of two-phase Fe-25Al-xZr alloys compared to three-phase Fe-30Al-xZr alloys. Metallurgical and Materials Transactions A, Vol. 45, No. 1, 2014, pp. 335-342.